This is the accepted manuscript made available via CHORUS. The article has been published as:

Multiscale Structure, Interfacial Cohesion, Adsorbed Layers, and Thermodynamics in Dense Polymer-Nanoparticle Mixtures

So Youn Kim, Kenneth S. Schweizer, and Charles F. Zukoski

Phys. Rev. Lett. **107**, 225504 — Published 22 November 2011

DOI: 10.1103/PhysRevLett.107.225504

Physical Review Letters, 2nd Revised, Sep, 2011

Multiscale Structure, Interfacial Cohesion, Adsorbed Layers and Thermodynamics in Dense Polymer-Nanoparticle Mixtures

So Youn Kim,[1] Kenneth S. Schweizer[1-3*] and Charles F. Zukoski[1-4*]

[1]Department of Chemical & Biomolecular Engineering, [2]Department of Materials Science, [3]Frederick Seitz Materials Research Laboratory, University of Illinois, Urbana, IL 61801, USA, [4]Science and Engineering Research Council, Agency for Science Technology and Research, Singapore

[*] E-mail: czukoski@illinois.edu, kschweiz@illinois.edu

PACS numbers : 61.46.Df, 61.41.+e, 61.05.fg

Abstract

We establish the existence and size of adsorbed polymer layers in miscible dense nanocomposites and their consequences on microstructure and the bulk modulus. Using contrast matching small angle neutron scattering to characterize all partial collective structure factors of polymers, particles and their interface, we demonstrate qualitative failure of the random phase approximation, accuracy of the polymer reference site interaction model theory, ability to deduce the adsorbed polymer layer thickness, and high sensitivity of the nanocomposite bulk modulus to interfacial cohesion.

Particle aggregation in concentrated polymer solutions, melts and crosslinked elastomers profoundly alters the mechanical, optical and electrical properties of nanocomposites [1-5]. Mechanisms of controlling the state of particle aggregation in these complex mixtures remain elusive and poorly understood [6]. Conceptual frameworks for achieving good dispersion generally rely on chemically or physically bound polymer layers [7, 8] to induce a repulsive interparticle potential-of-mean-force between nanoparticles [9, 10]. Nonetheless, understanding the nature of, and what controls, the structure and properties of these layers remains an outstanding challenge in soft matter of broad importance in polymer science, colloid science, and even biological systems. Obstacles limiting progress include (i) developing experimental tools and physics-based strategies for measuring and controlling the material-specific strength of polymer segments-particle surface attraction, (ii) differentiating polymer segments adsorbed on the nanoparticle surface from bulk polymer in the dense polymer solutions or melts, and (iii) measuring the packing structure of *both* segments and particles over a wide range of length scales and volume fractions.

In this Letter we present experimental results addressing the above issues using contrast matching small angle neutron scattering techniques in conjunction with carefully designed, thermodynamically stable (miscible) concentrated ternary solutions of short chain polymers (oligomers), nanoparticles and solvent. Measuring the intensity of scattered neutrons as a function of particle and polymer scattering contrast allows determination of all three partial collective structure factors that quantify spatially-resolved segment-segment, particle-particle, and interfacial concentration fluctuations [11]. We employ this experimental knowledge to : (i) determine the adsorbed layer

thickness, (ii) quantitatively test at an unprecedented level the microscopic Polymer Reference Interaction Site Model (PRISM) theory [12,13], and (iii) discover strong limitations of the incompressible random phase approximation (IRPA) [14]. How interfacial cohesion can qualitatively modify the effect of particle addition on the nanocomposite bulk modulus is addressed based on the experimentally validated theory.

Silica nanoparticles of diameter D=40nm are synthesized via the standard Stöber process [15] and suspended in dense polymer solutions composed of oligomeric poly(ethylene glycol) (PEG) of molecular weight 400 (27 backbone bonds, 9 monomers) and D_2O and H_2O solvents. Oligomer concentration is described by the ratio of PEG to PEG plus solvent volumes (R_{PEG}) which is fixed at a high value of 0.45 which ensures physical behavior representative of melts since the monomer collective density fluctuation correlation length is of order the segment size, a nm. Silica volume fraction (ϕ_c) is varied from 0.05 to 0.30. All experiments are performed at room temperature, and we find no evidence of aggregation or phase separation. Intensities of scattered neutrons were measured in the range of $0.004<q<0.04$ Å^{-1} which corresponds to a reduced wave vector range of $1.6<qD<13$ or $0.03<qd<0.3$ where $d \sim 0.6$ nm is the monomer size. Due to the small values of qd probed, the polymer segment form factor is set to unity. The intensity, $I(q)$, of scattered neutrons at wave vector q has three contributions:

$$I(q) = n_c \Delta\rho_c^2 P_c(q) S_{cc}(q,\phi_c) + 2\Delta\rho_c \Delta\rho_p \sqrt{n_c n_p P_c(q)} S_{pc}(q) + n_p \Delta\rho_p^2 S_{pp}(q) \quad (1)$$

where $n_j = \rho^*_j V_j^2$, and ρ^*_j and V_j are number density and unit volume of the j^{th} component, respectively. $\Delta\rho_j$ is the difference of scattering length density of component j and the medium, $P_c(q)$ is the particle form factor, and $S_{ij}(q)$ are the collective concentration

fluctuation structure factors associated with two components (*pp, pc, cc*) where the subscript *p (c)* indicates oligomer segments (particles).

To extract all three $S_{ij}(q)$ at a fixed ϕ_c, ρ_j is determined as a function of D_2O/H_2O ratio in the solvent phase and the $\Delta\rho_j$ are changed by appropriately varying the D_2O/H_2O ratio [11]. The quantities n_c and n_p are determined from the mass concentrations and size of the silica particles and oligomer segments for each sample. Choosing an D_2O/H_2O ratio where $\Delta\rho_p$=0, Eq. (1) is simplified to $I(q)=n_c\Delta\rho_c^2P_c(q)S_{cc}(q,\phi_c)$. This allows determination of $P_c(q)$ at low ϕ_c =0.03 where interparticle correlations are absent ($S_{cc}(q,\phi_{c,low})$=1) as shown in the lower inset of Fig.1. $S_{cc}(q)$ is obtained by dividing the scattering intensity from the concentrated particle suspension (Fig. 1 for ϕ_c=0.2) by its dilute limit analog: $S_{cc}(q,\phi_c)=\frac{I(q,\phi_c)}{n_{c,low}\Delta\rho_c^{\,2}P(q)}\frac{n_{c,low}}{n_c}$ [11]. After these steps, at a particular D_2O/H_2O ratio, Eq.(1) is simplified to $I_k(q)=a_k+b_kS_{pc}(q)+c_kS_{pp}(q)$ where the only unknowns are $S_{pp}(q)$ and $S_{pc}(q)$, and a_k and b_k are known q-dependent constants and c_k is a known q-independent constant where the subscript k denotes the D_2O ratio. We solve these simultaneous equations via multiple linear regression fitting methods using $I(q)$ measured at 3 D_2O/H_2O ratios corresponding to $\Delta\rho_c$~0 and two intermediate values close to $\Delta\rho_c$=0, which thereby yields $S_{pp}(q)$ (upper inset of Fig. 1) and $S_{pc}(q)$. Additional technical details of secondary importance are given in [11].

Scattering patterns are compared with the standard polymer nanocomposite version of PRISM integral equation theory where the solvent enters implicitly, details of which are thoroughly documented in the literature and Supplementary Material [11-13, 16-19]. All species interact via pair decomposable site-site hard core repulsions. The

chemical nature of the mixture enters via an exponential monomer-particle interfacial attraction, $U_{pc}(r) = -\varepsilon_{pc} \exp\left(-(r-(D+d)/2)/\alpha d\right)$, where ε_{pc} is the net energy decrease to transfer a segment (diameter, d) of the freely jointed chain from a concentrated polymer solution environment to the nanoparticle surface (diameter, D), and α=0.5d is the spatial range. Predictions of the theory are weakly dependent on chain length (N), and N=100 is used as a representative of the *equilibrium* behavior of both oligomers (N~10) and long chain polymers [19]. This provides theoretical support for our belief based on general physical considerations for dense polymer liquids that our present oligomer-based system behaves similarly to its equilibrated long chain analog. Real space intermolecular site-site pair correlations, $g_{ij}(r)$, are computed by solving three coupled nonlinear integral equations, from which the $S_{ij}(q)$ directly follow [11,18].

Experimental partial structure factors at ϕ_c=0.2 are shown in Fig.1. $S_{cc}(q)$ has a form characteristic of a correlated fluid, and both $S_{cc}(q)$ and $S_{pp}(q)$ display peaks near qD~ 4-6. The peak in $S_{cc}(q)$ is associated with a liquid-like nanoparticle packing, while the intense "microphase-like" peak in $S_{pp}(q)$ occurs at a length scale which greatly exceeds that of the PEG radius-of-gyration corresponding to $qD=2\pi D/R_g$~360. Its physical origin is spatial correlations between adsorbed polymers with non-bulk-like properties mediated by nanoparticles [12]. In the following we use the $S_{ij}(q)$ to both quantitatively test PRISM theory and demonstrate, for the first time, that based on a single volume fraction independent value for ε_{pc} all three partial structure factors can be understood, and such information allows the experimental measurement of the existence and thickness of an adsorbed polymer layer.

Figure 1 compares the experimental $S_{cc}(q)$ and $S_{pp}(q)$ with theoretical calculations for interfacial attraction strengths: $0.25\ kT < \varepsilon_{pc} < 1.05\ kT$. For both structure factors, note the high sensitivity of the predicted scattering patterns to the value of ε_{pc}. Good agreement between theory and experiment is found for both $S_{cc}(q)$ and $S_{pp}(q)$ with a common value of $\varepsilon_{pc} = 0.45kT$, very close to the value of $\varepsilon_{pc} = 0.55kT$ previously deduced for $S_{cc}(q)$ of *pure melts* of silica and PEG [18]. Most significantly, the accuracy of PRISM theory for predicting collective *polymer* microstructure with no adjustable parameters is demonstrated for the first time. Excellent theory-experiment agreement is also found for the cross fluctuations, $S_{pc}(q)$ [11].

The measured and predicted $S_{ij}(q)$ at all volume fractions studied are presented in Fig. 2; the theoretical results employ the *same* value of ε_{pc}=0.45kT. Increasing ϕ_c suppresses long wavelength nanoparticle concentrations fluctuations, but enhances low wave vector polymer fluctuations. The increased height and shift of the first peak in $S_{cc}(q)$ indicates a more ordered first neighbor shell, while increased coherency of segment density fluctuations on the nanoparticle length scale is deduced from the form of $S_{pp}(q)$. Significant quantitative deviation between theory and experiment occurs for $S_{pp}(q)$ in the peak region at ϕ_c=0.3, perhaps suggestive that PRISM theory over predicts adsorbed polymer density at high nanoparticle concentration. The upper right inset shows the cross partial structure factors are negative, and with increasing wave vector, $S_{pc}(q)$ decreases and goes through a minimum at qD~4-6. These features indicate anti-correlation of particle and polymer segment concentration fluctuations over a wide range of length scales. As ϕ_c increases, the minimum in $S_{pc}(q)$ grows in magnitude and occurs at larger qD, tracking the increased local interparticle correlation and growth of the $S_{pp}(q)$ peak.

Taken together, there is remarkable qualitative and near quantitative agreement between *all three* experimental structure factors and PRISM theory over a wide range of wave vectors and all volume fractions based on a *single, volume fraction independent* value of ε_{pc}. This provides significant support for the intrinsic material origin of ε_{pc}, the dominance of the interfacial attraction strength in determining both polymer and particle microstructures, and the accuracy of PRISM theory for the full mixture structure.

Often the structure of multi-component polymeric materials (blends, block copolymers) on length scales well beyond the monomer scale is accurately described by the incompressible random phase approximation (IRPA) [14, 20]. The IRPA predicts inter-relations between the three partial collective structure factors: $S_{RPA}(q) = \rho_c K_{cc} S_{cc}(q) = \rho_p K_{pp} S_{pp}(q) = (\rho_c \rho_p)^{0.5} K_{pc} S_{pc}(q)$, where $K_{ij} = v_i v_j / (\phi_t (v_p v_c)^{1/2})$, v_i is the site volume of species i, ρ_i is the number density of component, i and ϕ_t is the total mixture packing fraction [20]. The total density fluctuation structure factor, $S_{tot}(q) = \rho_c K_{cc} S_{cc}(q) + \rho_p K_{pp} S_{pp}(q) - 2(\rho_c \rho_p)^{0.5} K_{pc} S_{pc}(q)$, is zero by assumption. Traditionally, the IRPA is applied to dense polymeric systems where attractions are weak and structural differences between species small. However, its validity is unknown for polymer nanocomposites where attractions can be strong, there is a massive length scale asymmetry, and the packing polymers at hard curved internal surfaces is relevant. Our measurement of all three $S_{ij}(q)$ allows the first critical testing of the validity of the IRPA for polymer nanocomposites.

The IRPA predicts the peaks in S_{pp}, S_{cc} and S_{pc} should all occur at the same value of qD. As shown in the inset to Fig. 3, at a constant nanoparticle volume fraction there are systematic, ϕ_c-dependent differences in the peak locations. The main frame of Fig. 3 shows $S_{tot}(q)$ at each ϕ_c. For $qD<4$, the total density fluctuations do reach a q-independent

(but non-negligible) constant which, however, varies significantly with nanoparticle volume fraction. For shorter wavelength density fluctuations ($qD > 4$), but still long compared to monomer and oligomer sizes, the total density fluctuations depend on length scale, and grow strongly with ϕ_c. Thus, the strong packing asymmetry of the oligomers and particles induces total density fluctuations of significant magnitude and spatial variation which results in strong *qualitative* deviations from the IRPA relations.

To both shed more light on the origins of the IRPA failure, and to in situ characterize adsorbed polymer layers, we consider scattering in a system where $\Delta\rho_c=0$ and hence the intensity is due to non-bulk-like polymer concentration fluctuations from shells of adsorbed polymer. The scattered intensity in Eq. (1) can then be approximated as $\sim S_{pp}(q) \sim S_{pp}^*(q) P_s(q)$, where $P_s(q)$ is the $\phi_c \rightarrow 0$ polymer shell form factor, and $S_{pp}^*(q)$ is the structure factor associated with correlations between the shell centers-of-mass (CM). Both $P_s(q)$ and $S_{pp}^*(q)$ can vary with shell volume fraction [21]. We argue that the adsorbed polymer shell CM will, to a good approximation, have the same correlations as experienced by the CM of the nanoparticles ($S_{pp}^*(q) \sim S_{cc}(q)$) such that when $\Delta\rho_c=0$, $I(q) \sim S_{pp}(q) \sim C S_{cc}(q) P_s^*(q)$, where C is a ϕ_c–dependent normalization constant.

Figure 4 presents the experimental $P_s^*(q)$ obtained from $S_{pp}(q)/S_{cc}(q)$, and the PRISM theory analog determined in the same manner. One notes $P_s^*(q)$ results from well-defined adsorbed oligomer layers that are structurally distinct from bulk polymers. The resulting $P_s^*(q)$ overlap well, with the first minimum shifting to slightly lower q as ϕ_c increases. Using scattering length density parameters at a match condition and a core-shell model form factor [22], the adsorbed shell thickness is determined [11] to be ~0.7-1 nm, which is modestly larger than the PEG segment length. It is notable that the signature

of an adsorbed layer with non-bulk density fluctuations is accurately captured by PRISM theory (solid curve). Our results demonstrate the failure of IRPA arises largely from polymer adsorption which alters local oligomer segment concentration fluctuations. Moreover, $S_{pp}(q)$ and $S_{pc}(q)$ contain critical information that allows determination of adsorbed layer thickness under dense conditions. Note also that as ϕ_c increases, the data suggests the oligomer layer thickness decreases weakly from ~1.1 to ~0.9 nm, presumably due to greater confinement.

Finally, we consider an important material property based on the experimentally validated theory, the nanocomposite bulk modulus, K_B ,which depends on the full mixture microstructure [18]. Figure 5 shows calculations of K_B normalized to its pure polymer melt analog, K_{B0}, over a wide range of interface attraction strengths. At higher ε_{pc} where adsorbed layers are well-developed and polymers mediate repulsive interparticle interactions, K_B decreases with increasing ϕ_c, consistent with prior theoretical studies [18, 23], and seemingly a recent measurement of the thermal pressure coefficient (proportional to K_B) in a polymer nanocomposite [24]. However, for smaller ε_{pc} where polymers adsorb less, and repulsive and attractive (entropic depletion) effects coexist in the nanoparticle potential-of-mean force [12, 13], the bulk modulus increases with particle loading. Hence, we predict a direct connection between changes of polymer organization around nanoparticles and mixture microstructure with nanocomposite stiffness. Crucial to this rich behavior is that the total mixture volume fraction varies with ϕ_c in a manner consistent with melt and concentrated solution experiments [16, 18]. The striking prediction [25] that lowering ε_{pc} towards the depletion demixing boundary stiffens the nanocomposite, while increasing the attraction strength away from it results

in softening, provides a new route to controlling the bulk modulus based on rational manipulation of polymer-particle interfacial cohesion and nanoparticle concentration.

In summary, using contrast matching neutron scattering we have measured and compared to the theory, for the first time, all collective partial structure factors in concentrated oligomer-nanoparticle mixtures. Polymer and particle concentration fluctuations, and their cross-correlation, are all well predicted by PRISM theory based on a single key parameter, the segment–particle interfacial attraction strength. We developed a novel way to measure the thickness of an adsorbed layer in dense polymer solutions, and demonstrated that nanoparticle miscibility correlates with the existence of nm-thick adsorbed polymer layers that provide steric stability. We also discovered large qualitative failures of the IRPA. Broader implications of our results lie in our demonstration that, by altering the magnitude of ε_{pc} through changes in particle surface chemistry and/or polymer chemistry, the microstructure of nanocomposites and concentrated polymer solutions can be tuned to achieve desired goals.

Acknowledgements

This work was supported by the Nanoscale Science and Engineering Initiative under NSF Award DMR-0642573. We acknowledge the support of the National Institute of Standards and Technology, U.S. Department of Commerce, in providing the neutron research facilities used in this work. We deeply appreciate helpful discussions with Dr. Lisa Hall, who also kindly provided codes for the theoretical calculations.

References

[1] P. M. Ajayan, L. S. Schadler, and P. V. Braun, *Nanocomposite Science and Technology* (Wiley-VCH, Weinheim, 2003).

[2] M. J. Wang, Rubber Chem. Technol. **71**, 520 (1998).

[3] J. Oberdisse, P. Hine, and W. Pyckhout-Hintzen, Soft Matter **3**, 476 (2007).

[4] J. Oberdisse, Soft Matter **2**, 29 (2006).

[5] P. Rittigstein *et al.*, Nat. Mater. **6**, 278 (2007).

[6] L. Khounlavong, V. Pryamitsyn, and V. Ganesan, J. Chem. Phys. **133** (2010).

[7] V. Ganesan, C. J. Ellison, and V. Pryamitsyn, Soft Matter **6**, 4010 (2011).

[8] P. Akcora *et al.*, Nat. Mater. **8**, 354 (2009).

[9] M. E. Mackay *et al.*, Science **311**, 1740 (2006).

[10] J. A. Pomposo *et al.*, Macromol.Rapid Comm. **32**, 573 (2011).

[11] See supplementary materials available online

[12] L. M. Hall, and K. S. Schweizer, J. Chem. Phys **128**, 234901 (2008).

[13] J. B. Hooper, and K. S. Schweizer, Macromolecules **38**, 8858 (2005).

[14] P. G. De Gennes, *Scaling Concepts in Polymer Physics* (Cornell University Press, Ithaca, 1979).

[15] W. Stober, A. Fink, and E. Bohn, J. Colloid Interf. Sci. **26**, 62 (1968).

[16] S. Y. Kim *et al.*, Macromolecules **43**, 10123 (2010).

[17] K. S. Schweizer, and J. G. Curro, Adv. Chem. Phys **98**, 1 (1997).

[18] L. M. Hall *et al.*, Macromolecules **42**, 8435 (2009).

[19] Since the total density fluctuation correlation length in the dense mixture is short, one expects on general physical grounds that the structure, scattering patterns, miscibility and thermodynamics are all weakly dependent on chain length under equilibrium conditions. This expectation agrees with prior PRISM theory studies which find mixtures with N=10 chains behave significantly differently than N=1 solvents, and quite similarly to the long chain limit. Hence, we expect the oligomer PEG 400 (N~10) will behave quite similarly as its long chain "polymer" analog under equilibrated conditions.

[20] J. G. Curro, and K. S. Schweizer, Macromolecules **24**, 6736 (1991).

[21] D. Qiu, C. Flood, and T. Cosgrove, Langmuir **24**, 2983 (2008).

[22] A. Guinier, and G. Fournet, *Small-Angle Scattering of X-Rays* (John Wiley and Sons, New York, 1955).

[23] A. L. Frischknecht, E. S. McGarrity, and M. E. Mackay, J. Chem. Phys **132**, 204901 (2010).

[24] K. Z. Win *et al.*, J. Appl. Polym. Sci. **116**, 142 (2010).

[25] As might be physically anticipated based on consideration of polymer packing in interstices between particles, preliminary calculations find the precise behavior depends on nanoparticle size, and weakly on interfacial attraction range. A detailed study will be presented elsewhere, but a key finding is that bulk modulus softening is a nanoscale phenomenon which does not occur if particles are sufficiently large whence PRISM theory predicts particle addition increases the modulus per continuum arguments.

[26] S. R. Kline, J. Appl. Cryst. **39**, 895 (2006).

Figure caption

Figure 1. (Color online) Nanoparticle collective structure factor as a function of reduced wave vector at ϕ_c=0.2. Experimental data are shown as squares, and PRISM theory calculations as curves which illustrate the effect of changing the segment-nanoparticle attraction strength, ε_{pc}. (Lower inset) Scattered intensity at ϕ_c=0.2 and 0.03 where $\Delta\rho_p$~0. (Upper inset) Corresponding collective polymer structure factor and theoretical calculations. Theory and experiment comparisons for the cross correlation structure factor, $S_{pc}(q)$, are given in [11].

Figure 2. (Color online) Polymer collective structure factor as a function of reduced wave vector at different nanoparticle volume fractions, ϕ_c, as indicated in legend. Corresponding smooth curves are the PRISM theory results for ε_{pc}=0.45kT. (Upper left inset) Nanoparticle collective structure factor, S_{cc}, under the same conditions. (Upper right inset) Cross fluctuation structure factor, S_{pc}, under the same conditions. Deviations between theory anhd experiment at qD~10-12 are likely due to the low intensity of the raw data which renders accurate of extraction of S_{pc} difficult. [11]

Figure 3. (Color online) Dimensionless total density fluctuation structure factor as a function of reduced wave vector at the different nanoparticle volume fractions, ϕ_c, indicated in legend. Corresponding smooth curves are the PRISM theory results for ε_{pc}=0.45kT. (inset) Positions of first (q^*D) and second peaks ($q^{**}D$) as a function of ϕ_c. Dots are experimental data and curves are the PRISM theory predictions with ε_{pc}=0.45kT.

Figure 4. (Color online) Adsorbed polymer shell form factor as a function of reduced wave vector. $P_s^*(q)$ is determined from PRISM theory (solid curve) and experiment (dots) at four volume fractions. The dash-dot line is a fit to the form factor of a core-shell model [22, 26]. The bare spherical-particle form factor, $P_c(q)$, is shown as the short dashed curve for comparison to $P_s^*(q)$, experimentally obtained from dilute particle suspensions and fitted to the standard homogeneous sphere model. Fitting equations are found in [11].

Figure 5. (Color online) PRISM theory calculations of the nanocomposite bulk modulus (normalized by its pure polymer melt value) for several values of interfacial attraction strength, ε_{pc}, which increases from 0.25 kT (top) to 1.05 kT (bottom).

Figure 1

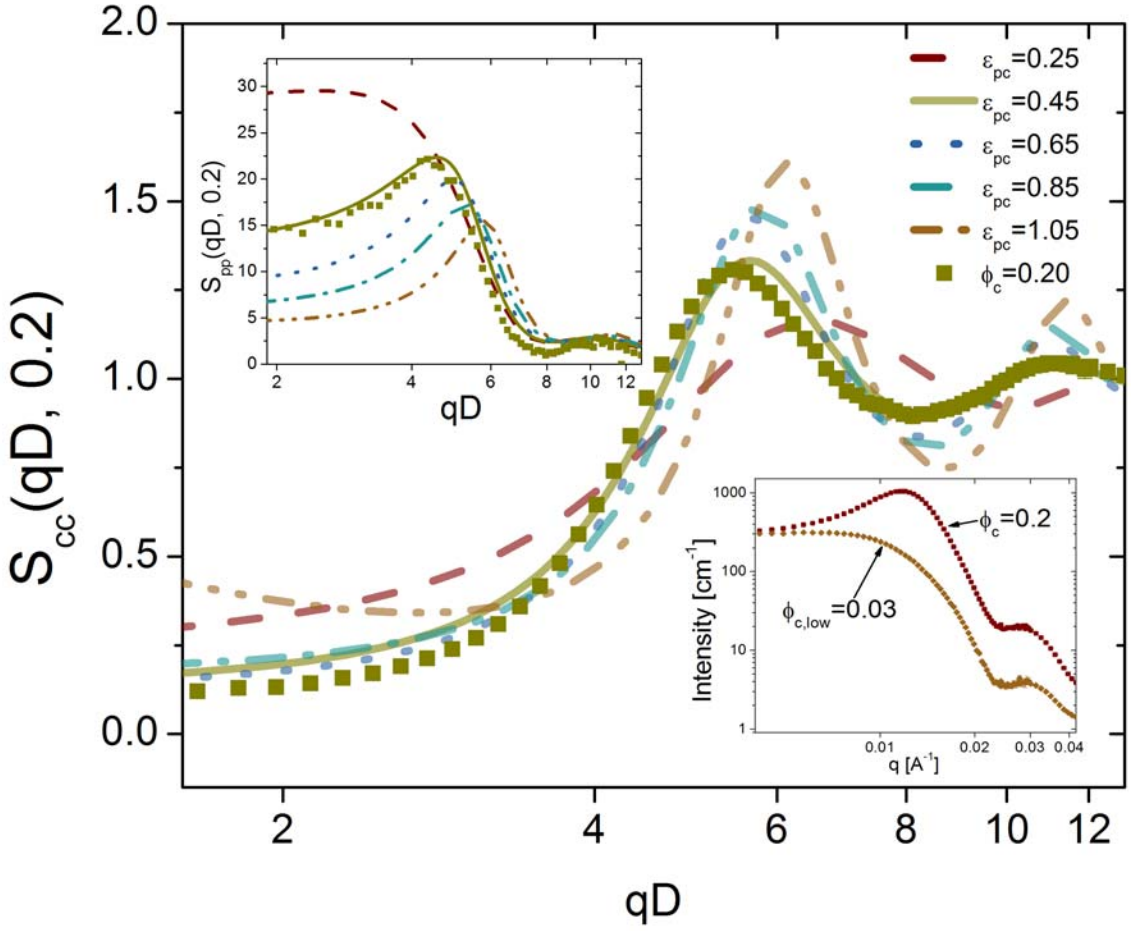
$S_{cc}(qD, 0.2)$
qD
ε_{pc}=0.25
ε_{pc}=0.45
ε_{pc}=0.65
ε_{pc}=0.85
ε_{pc}=1.05
ϕ_c=0.20
$S_{pp}(qD, 0.2)$
qD
Intensity [cm^{-1}]
ϕ_c=0.2
$\phi_{c,low}$=0.03
q [A^{-1}]

Figure 2

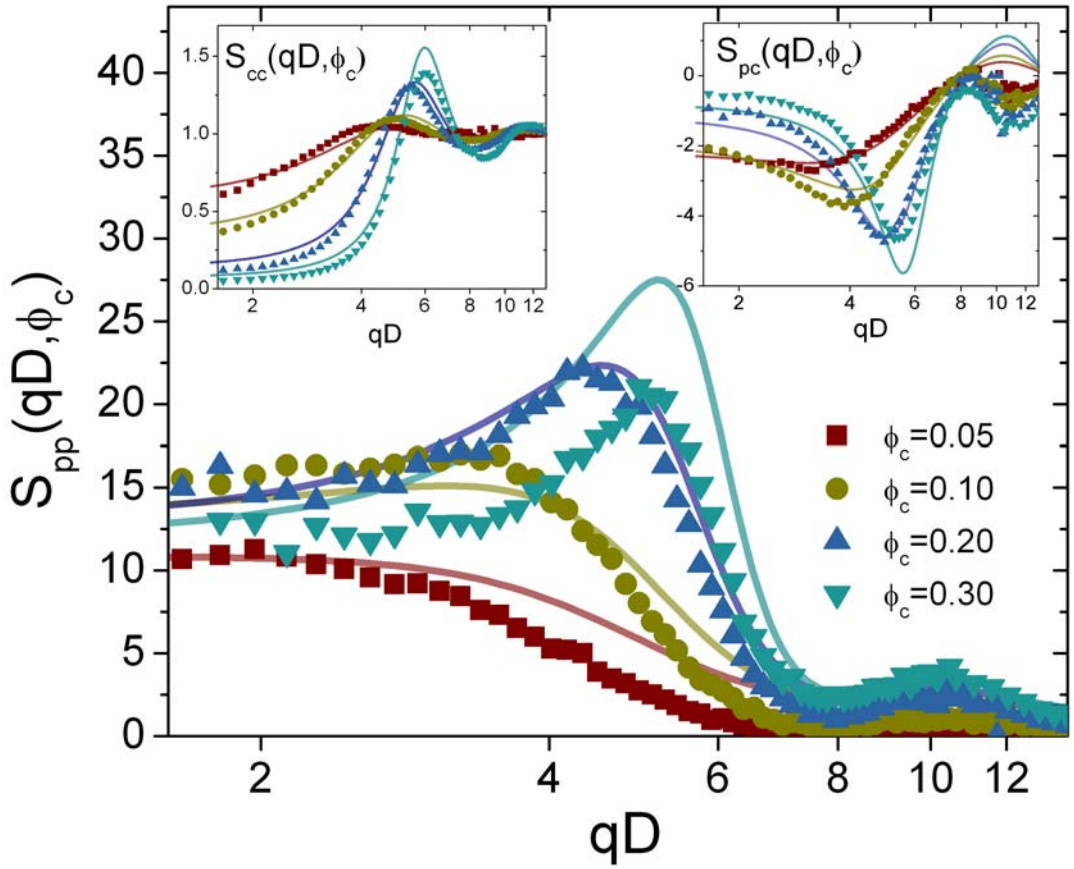
$S_{pp}(qD,\phi_c)$
qD
ϕ_c=0.05
ϕ_c=0.10
ϕ_c=0.20
ϕ_c=0.30
$S_{cc}(qD,\phi_c)$
$S_{pc}(qD,\phi_c)$

Figure 3.

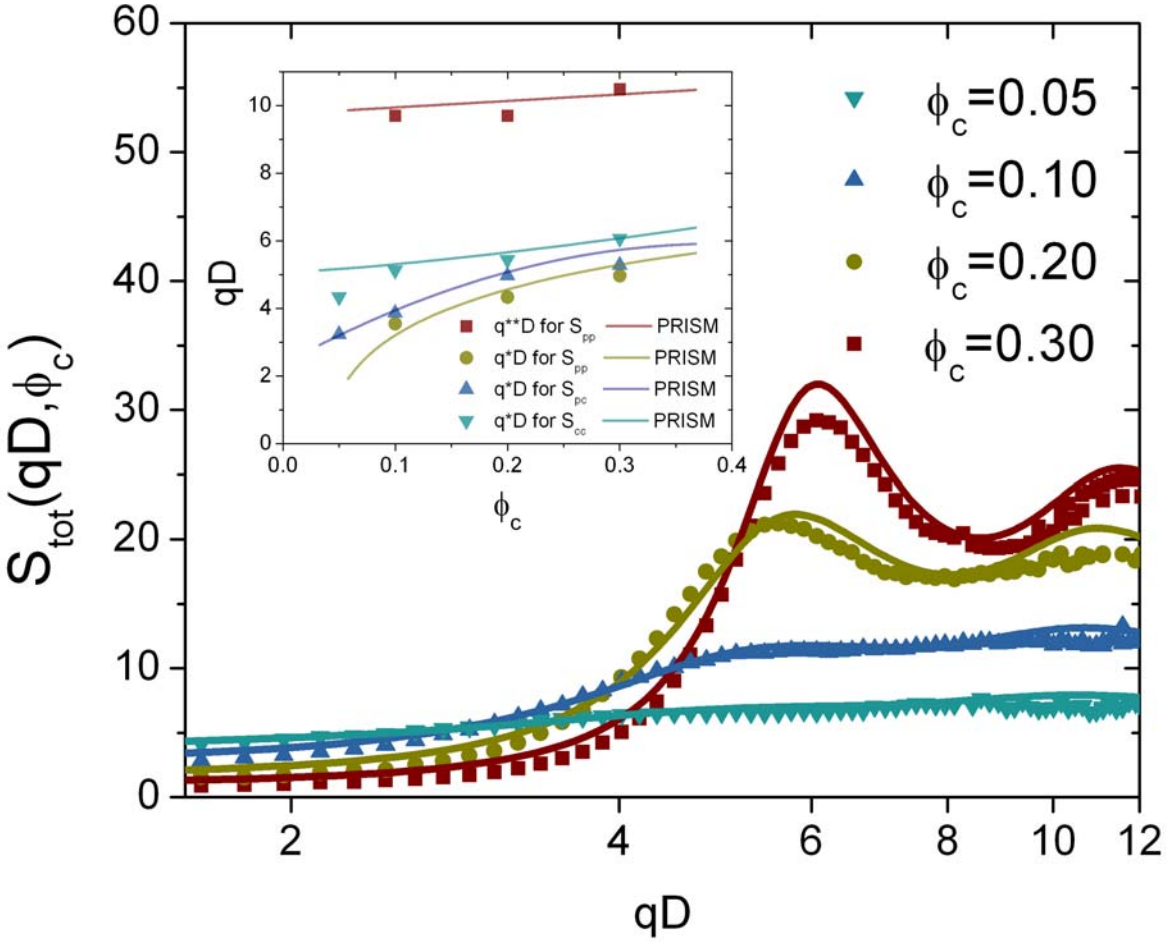
$S_{tot}(qD,\phi_c)$
qD
ϕ_c=0.05
ϕ_c=0.10
ϕ_c=0.20
ϕ_c=0.30
qD
ϕ_c
q**D for S_{pp}
q*D for S_{pp}
q*D for S_{pc}
q*D for S_{cc}
PRISM
PRISM
PRISM
PRISM

Figure 4

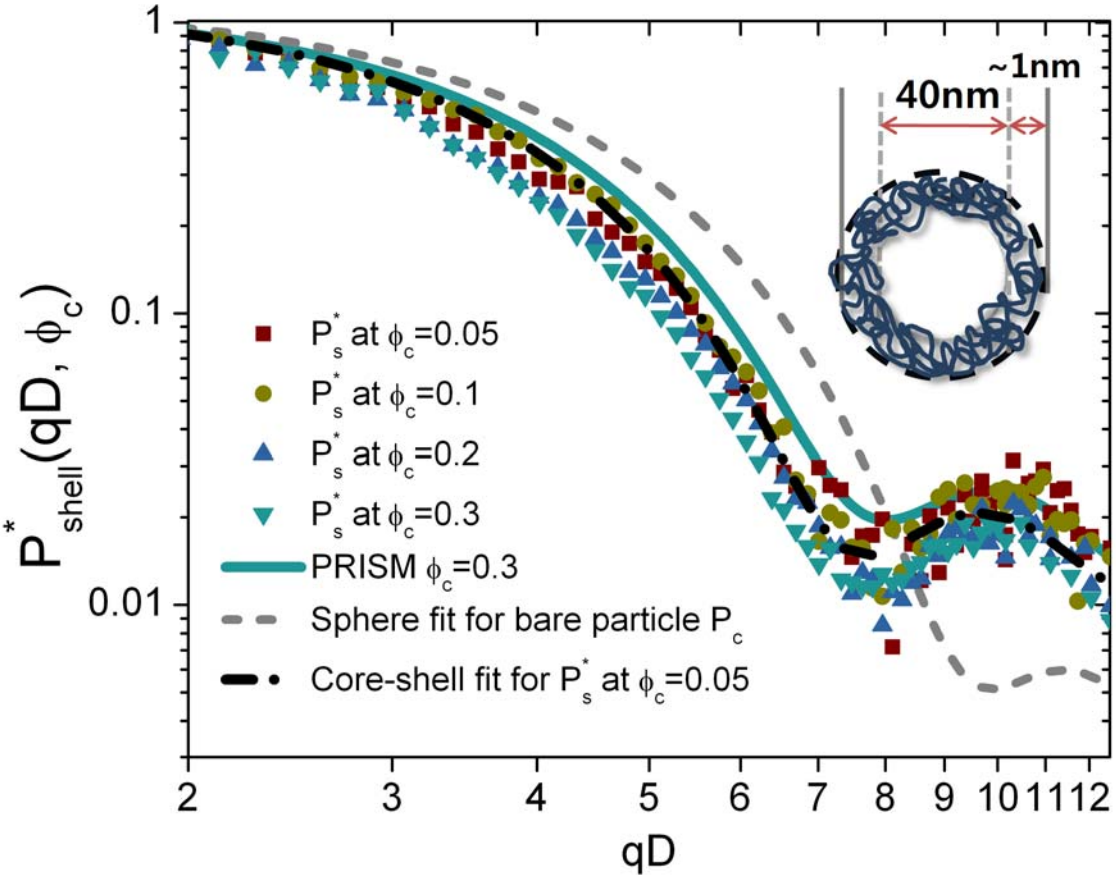
1
0.1
0.01
$P^*_{shell}(qD, \phi_c)$
2
3
4
5
6
7
8
9
10
11
12
qD
~1nm
40nm
P^*_s at ϕ_c=0.05
P^*_s at ϕ_c=0.1
P^*_s at ϕ_c=0.2
P^*_s at ϕ_c=0.3
PRISM ϕ_c=0.3
Sphere fit for bare particle P_c
Core-shell fit for P^*_s at ϕ_c=0.05

Figure 5

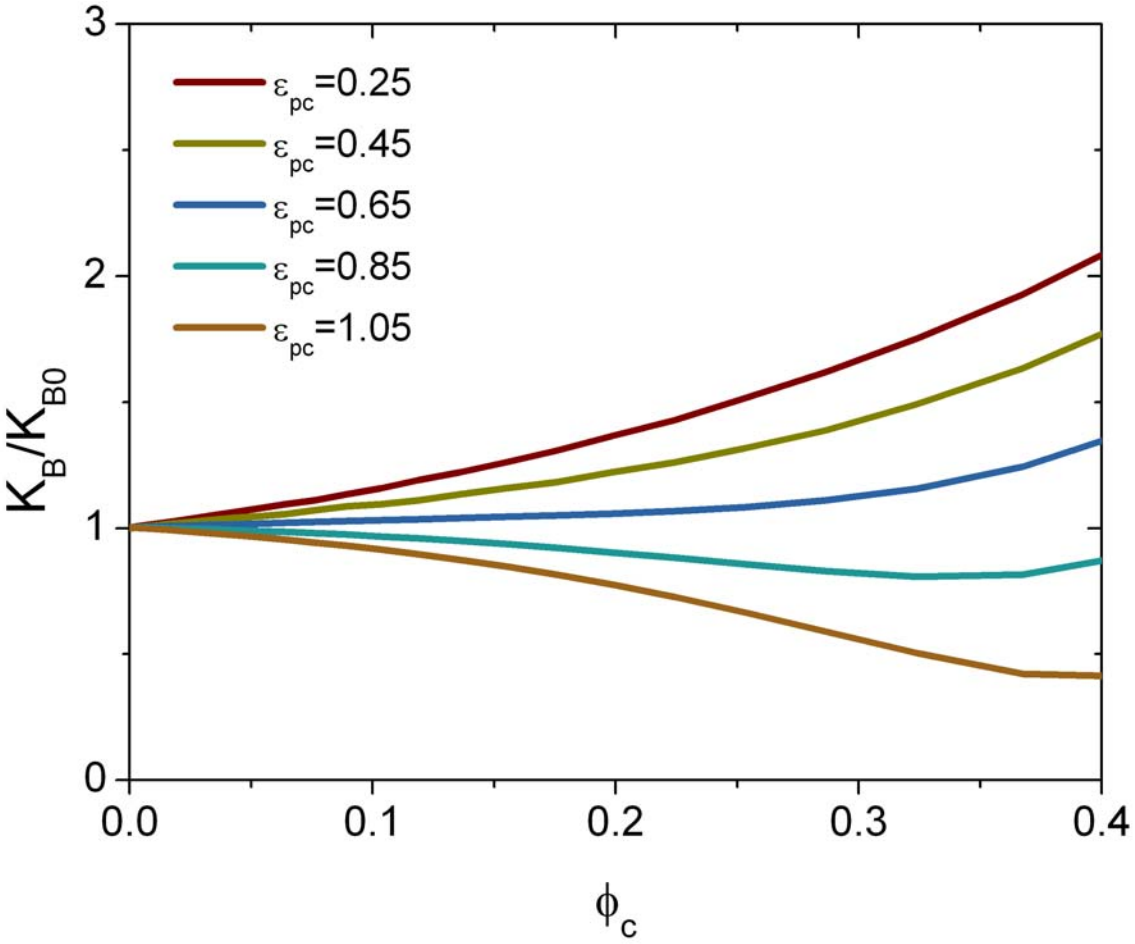
3
2
1
0
0.0
0.1
0.2
0.3
0.4
K_B/K_{B0}
ϕ_c
ε_{pc}=0.25
ε_{pc}=0.45
ε_{pc}=0.65
ε_{pc}=0.85
ε_{pc}=1.05